Magnetophonon resonance of quasi-two-dimensional and quasi-one-dimensional electronic systems in tilted magnetic fields

1998 J. Phys.: Condens. Matter 10 4659

(http://iopscience.iop.org/0953-8984/10/21/021)

J. Phys.: Condens. Matter **10** (1998) 4659–4676. Printed in the UK PII: S0953-8984(98)87912-5

Magnetophonon resonance of quasi-two-dimensional and quasi-one-dimensional electronic systems in tilted magnetic fields

Akira Suzuki and Masayuki Ogawa

Centre for Solid-State Physics and Department of Physics, Faculty of Science, Science University of Tokyo, 1-3 Kagurazaka, Shinjuku-ku, Tokyo 162-8601, Japan

Received 19 September 1997, in final form 12 February 1998

Abstract. We have studied the essential physics of magnetophonon resonances (MPR) in quasi-two-dimensional (Q2D) and quasi-one-dimensional (Q1D) electronic systems brought about by the electron confinement due to the electrostatic potentials and the magnetic confinement on tilting a perpendicular magnetic field. Qualitative features of the MPR effects, their physical origin, and the dimensional crossover between Q2D and Q1D systems associated with the confining potential in tilted magnetic fields are discussed in detail, on the basis of a simple model of parabolic confining potentials.

1. Introduction

Recently, the magnetophonon resonance (MPR) effect in low-dimensional systems [1–13] has received much attention from both the experimental and theoretical points of view, since the quantization of electron energies in Q2D and Q1D electron gas (EG) systems in the presence of a high magnetic field is different from that of a bulk (3DEG) system [14–18]. Moreover, a suitably directed magnetic field serves to add an extra confining potential to the initial electrostatic confinement and causes a dramatic change in the energy spectrum, leading to so-called hybrid magnetoelectric quantization. As a consequence, one would expect different behaviour of the MPR effects in such systems from the known MPR effects in 3DEG systems.

Many of the MPR theories for Q2DEG systems considered the case in which the magnetic field is applied normal to the Q2D electronic plane [6, 7, 9]. When the confinement is sufficiently tight and one can neglect the inter-sub-band transitions, the MPR condition for such Q2D systems is the same as that for a bulk (3D) system, since the two-dimensional constraint does not influence the cyclotron motion. However, in the case of a Q1D system [10–13], there exists an additional confining potential in the plane in which the electrons undergo cyclotron motion. Accordingly, this affects the Landau quantization. Therefore, MPR conditions in Q1D systems will be different from those in Q2D systems. Moreover, we can expect that if one applied a magnetic field at an arbitrary angle, a confining potential would appear in the new plane of the cyclotron motion. Thus we expect that this will affect the MPR conditions in the Q2D systems as well. Even in the same Q2D system, the resonance conditions would be different from the tight- and loose-confinement cases. In the case of a Q1D electronic system, a tilted magnetic field applied to the transverse direction of the Q1D quantum wire should influence the MPR condition in two ways. Not only are the

0953-8984/98/214659+18$19.50

energy spacings between sub-bands affected, but also an additional effective confinement potential is formed. Moreover, the angle dependence of the MPR in an asymmetric quantum wire would be different from that in a symmetric quantum wire.

The purpose of the present work is to investigate the MPR effects in Q1D and Q2D electronic systems in an effort to understand the qualitative behaviour of the MPR effects in such low-dimensional systems, on the basis of a simple parabolic model for the confinement potential. We shall derive the conductivity σ_{yy} for the Q1D/Q2D electronic system subjected to a tilted magnetic field and obtain MPR conditions as a function of the field strength (B), and tilt angle (θ) of the applied magnetic field $(\boldsymbol{B})$ as well as the strength parameters (ω_1 and/or ω_2) of the parabolic potentials, which characterize the strength of confinement of the Q1DEG and Q2DEG. We will investigate how the MPR effects are affected by the constraint due to the directionality of the applied magnetic fields. This gives an anomalous angular dependence of the field positions. We examine the dependence of the MPR on the strengths of the confining potentials (that is, the dimensionality difference between the Q2D and the Q1D systems). In the formulation of the problem, the single-particle picture has been used throughout this work, and thus the electron–electron interactions have been ignored. Although such interactions would be expected to affect the MPR linewidth considerably, they are not expected to change the overall MPR lineshape. We assume that the interaction with bulk LO phonons is the dominant scattering mechanism.

The rest of the paper is organized as follows. In section 2, an exactly solvable model for Q2D and Q1D electronic systems is presented in a unified manner. In section 3, general formulae for the transverse magnetoconductivity σ_{yy} and the relaxation rate $\Gamma/\hbar$ are given and are evaluated for the Q1D/Q2D model system subjected to a tilted magnetic field. We show that the transverse magnetoconductivity σ_{yy} for the Q2D/Q1D system consists of the usual Drude term arising from the drift motion of electrons, and hopping terms associated with MPR. In section 4, the relaxation rate, which is closely related to the MPR, is evaluated for bulk LO-phonon scattering in the Q1D/Q2D EG system. The MPR conditions for the model systems are given explicitly and the effects of tilted magnetic fields and the confining potential on the MPR are discussed. Here, special attention is given to the behaviour of the MPR lineshape, such as the appearance of subsidiary MPR peaks, the shift of these MPR peaks and a reduction in MPR amplitude. Physical analysis of the theoretical results obtained is given in section 5. Diagonalization of the Hamiltonian which contains the crossed term is presented in an appendix.

2. The model for Q2D and Q1D electronic systems in tilted magnetic fields

We consider the transport of an electron gas in a quantum-well structure and a quantum-wire structure. The Q2D electron gas is assumed to be confined to the x–y plane by an ideal parabolic potential $\frac{1}{2}m\omega_2^2z^2$ whereas the Q1D electron gas is assumed to be further confined in the x-direction by an additional parabolic potential $\frac{1}{2}m\omega_1x^2$ thus restricting free motion to the y-axis alone. In the presence of a magnetic field, the one-particle Hamiltonian (H_e) for such Q1D/Q2D electrons is expressed in a unified manner by

$$H_e = \frac{1}{2m}(\boldsymbol{p} + e\boldsymbol{A})^2 + V(x, z) \tag{2.1}$$

where $\boldsymbol{A}$ is a vector potential accounting for a constant magnetic field $\boldsymbol{B} = \boldsymbol{\nabla} \times \boldsymbol{A}$, m is the effective mass, and the confining potential $V(x, z)$ is given by

$$V(x, z) = \frac{1}{2}m\omega_1^2x^2 + \frac{1}{2}m\omega_2^2z^2. \tag{2.2}$$

We can see the dimensional crossover between the Q2D and the Q1D electronic systems (i.e., $\omega_1 \to 0$ for the Q2D electronic system) as well as the difference in the strength of each confinement on varying the confining-potential parameters (ω_1 and/or ω_2) in equation (2.2) for the Q1D/Q2D system. We shall consider the case in which the magnetic field $\boldsymbol{B}$ is applied in the transverse tilt direction to the wire/plane of the conductor: $\boldsymbol{B} = (B_x, 0, B_z) = (-B\sin\theta, 0, B\cos\theta)$. Here, the angle θ is measured from the z-axis in the x–z plane. To simplify the mathematics, we rotate the coordinates x and z by θ with respect to the y-axis so that the components of the applied $\boldsymbol{B}$ field in the new coordinates (x', y', z') can be expressed by $(B_{x'}, B_{y'}, B_{z'}) = (0, 0, B)$, with the Landau gauge $\boldsymbol{A} = (A_{x'}, A_{y'}, A_{z'}) = (0, Bx', 0)$. After the coordinate transformations $\{R_y(\theta)|(x, y, z) \mapsto (x', y', z')\}$, the one-particle Hamiltonian (2.1) for those confined (Q1D/Q2D) electrons subjected to the transverse tilted magnetic field can be expressed in the new Cartesian coordinates (x', y', z') as

$$H_e = \frac{1}{2m}[p_{x'}^2 + (p_{y'} + m\omega_c x')^2 + p_{z'}^2] + V(x', z') \tag{2.3}$$

where $V(x', z')$ is given by

$$V(x', z') = \frac{m}{2}\left[(\omega_1^2\cos^2\theta + \omega_2^2\sin^2\theta)x'^2 + (\omega_1^2\sin^2\theta + \omega_2^2\cos^2\theta)z'^2\right] + m(\omega_2^2 - \omega_1^2)\cos\theta\sin\theta x'z'. \tag{2.4}$$

Here, ω_c $(=eB/m)$ is the cyclotron frequency. It should be noted that the tilt angle θ of the applied $\boldsymbol{B}$-field is defined as $\theta = \tan^{-1}(B_x/B_z)$ and that the momentum component $p_{y'}$ is a constant of motion and can be written as $p_y = \hbar k_y$, where k_y is the quasi-continuous wave vector of motion parallel to the interfaces (that is, the wire/plane is in the y-direction ($\equiv$ the y'-direction). In this way, equation (2.1) along with equation (2.2) can be represented by two coupled harmonic oscillators as seen in equation (2.3) with equation (2.4). However, in the usual case in which $\omega_1, \omega_2 \ll \omega_c$, we can safely neglect the cross term $(\propto x'z')$ in equation (2.4) (see the appendix). Thus, equation (2.3) with equation (2.4) can be approximated as

$$H_e = \frac{p_{x'}^2}{2m} + \frac{m}{2}\Omega_{x'}^2(x' + x_0)^2 + \frac{p_{z'}^2}{2m} + \frac{m}{2}\Omega_{z'}^2 z'^2 + \frac{p_{y'}^2}{2\tilde{m}} \tag{2.5}$$

where $\Omega_{x'}$ and $\Omega_{z'}$ are respectively given by

$$\Omega_{x'} = \sqrt{\omega_1^2\cos^2\theta + \omega_2^2\sin^2\theta + \omega_c^2} \tag{2.6a}$$

$$\Omega_{z'} = \sqrt{\omega_1^2\sin^2\theta + \omega_2^2\cos^2\theta} \tag{2.6b}$$

and a renormalized effective mass $\tilde{m}$ is given by

$$\tilde{m} = m\left(1 - \frac{\omega_c^2}{\Omega_{x'}^2}\right)^{-1}. \tag{2.7}$$

The Hamiltonian (2.5) expressed in the new Cartesian coordinates is basically the Hamiltonian for two independent 1D simple harmonic oscillators, one with the effective (renormalized) cyclotron frequency $\Omega_{x'}$ in the x'-direction and the other with the effective confinement (sub-band) frequency $\Omega_{z'}$ in the z'-direction. In other words, those confined (Q1D/Q2D) electrons feel the effective potential $m\Omega_{x'}^2(x' + x_0)^2/2 + m\Omega_{z'}^2 z'^2/2$, where x_0 is given by

$$x_0 = \frac{\omega_c p_{y'}}{m\Omega_{x'}^2} \equiv \frac{\hbar\omega_c k_{y'}}{m\Omega_{x'}^2}. \tag{2.8}$$

The last term in equation (2.5) represents the y-component of the kinetic energy of a confined electron but with a field-dependent renormalized mass $\tilde{m}$ with respect to the effective mass m. Due to the presence of the confining potentials and/or the tilted magnetic field, the effective mass $\tilde{m}$ is increased by a factor $(1-\omega_c^2/\Omega_{x'}^2)^{-1}$, which depends on a tilt angle θ, the cyclotron frequency ω_c, and the confining-potential parameters (ω_1, ω_2) characterizing the dimensionality of the system.

The normalized eigenfunctions and eigenenergies of the one-electron Hamiltonian (2.5) are given by

$$\langle \boldsymbol{r}|\alpha\rangle \equiv \langle x', y', z'|n, l, k_{y'}\rangle = \frac{1}{\sqrt{L_y}}\varphi_n(x'+x_0)\mathrm{e}^{\mathrm{i}k_{y'}y'}\varphi_l(z') \tag{2.9}$$

and

$$\varepsilon_\alpha \equiv \varepsilon_{n,l,k_{y'}} = \left(n+\frac{1}{2}\right)\hbar\Omega_{x'} + \left(l+\frac{1}{2}\right)\hbar\Omega_{z'} + \frac{\hbar^2 k_{y'}^2}{2\tilde{m}} \qquad n, l = 0, 1, 2, \ldots \tag{2.10}$$

respectively. In equation (2.9), $\varphi_n(x'+x_0)$ and $\varphi_l(z')$ denote 1D simple-harmonic-oscillator wave functions with centres of the oscillation at $x' = -x_0$ and $z' = 0$, respectively, given by

$$\varphi_n(x'+x_0) = \sqrt{\frac{1}{\pi^{1/2}2^n n! l_{x'}}}\mathcal{H}_n\left(\frac{x'+x_0}{l_{x'}}\right)\exp\left[-\frac{1}{2}\left(\frac{x'+x_0}{l_{x'}}\right)^2\right] \tag{2.11a}$$

$$\varphi_l(z') = \sqrt{\frac{1}{\pi^{1/2}2^l l! l_{z'}}}\mathcal{H}_l\left(\frac{z'}{l_{z'}}\right)\exp\left[-\frac{1}{2}\left(\frac{z'}{l_{z'}}\right)^2\right] \tag{2.11b}$$

where $\mathcal{H}_n(x)$ denotes a Hermite polynomial [19], $l_{x'} = \sqrt{\hbar/m\Omega_{x'}}$ and $l_{z'} = \sqrt{\hbar/m\Omega_{z'}}$. The states of the Q1D/Q2D system are specified by two indices n, l and the wave vector $k_{y'}$ ($\equiv k_y = p_y/\hbar$), which govern the full energy spectrum given in equation (2.10). The wave function $\exp(\mathrm{i}k_y y)$ in equation (2.9) expresses a free motion in the y-direction (i.e., the y'-direction). The dimensions of the sample are assumed to be $V = L_x L_y L_z$. As shown in equation (2.10), the energy spectrum for the present Q1D and Q2D systems is *hybrid* quantized due to the presence of the tilted magnetic field and the electrostatic confining potential (2.2). The set of quantum numbers is designated by (n, l, k_y), where n and l denote the effective Landau (magnetic) and sub-band (electrostatic) level indices, respectively. We note that the dimensional crossover can be seen in the energy spectrum by simply varying the confining-potential parameters; $\omega_1 \to 0$ for the Q2DEG system and $\omega_1, \omega_2 \to 0$ for the 3DEG system. It is interesting that the dependence of the energy spectrum in equation (2.10) on the confining-potential parameters (ω_1, ω_2), the magnetic field direction (θ), and the magnitude of the applied magnetic field (B) has an important effect on the MPR effects for the Q1D/Q2D electronic system.

In the following treatment, we assume that the vibrational (phonon) spectra in the Q1D/Q2D system are identical with those in a bulk material, i.e., that the phonons, to a first approximation, are not affected by the heterojunctions forming quantum-wire and quantum-well structures. Deviations from this bulk behaviour, such as interface modes or slab modes, are neglected. The electron–phonon interaction Hamiltonian is then generally expressed by [20–22]

$$H_{e-ph} = \sum_{\boldsymbol{q}}[\gamma_{\boldsymbol{q}}(\boldsymbol{r})b_{\boldsymbol{q}} + \gamma_{\boldsymbol{q}}^\dagger(\boldsymbol{r})b_{\boldsymbol{q}}^\dagger] \tag{2.12}$$

where b_q and $b_q^\dagger$ are, respectively, the annihilation and creation operators for phonons with wave vector $\boldsymbol{q}$ and energy $\hbar\omega_q$, and the single-electron interaction operator $\gamma_q(\boldsymbol{r})$, which should be defined in terms of the matrix elements referring to electron states, is given by

$$\gamma_q(\boldsymbol{r}) = C(\boldsymbol{q}) \exp(\mathrm{i}\boldsymbol{q} \cdot \boldsymbol{r}). \tag{2.13}$$

Here, $C(\boldsymbol{q})$ is the Fourier transform of the electron–phonon interaction potential.

3. Magnetoconductivity associated with relaxation rates

In this section, an analytical expression of the transverse dc magnetoconductivity σ_{yy} for the model systems described in the previous section is developed by using the Kubo-type formula for a non-linear dc conductivity obtained previously [21]. For weak electric fields $\boldsymbol{E} = E\hat{\boldsymbol{y}}$ and weak interaction potentials, the Kubo-type formula for the non-linear conductivity $\sigma_{rs}(E)$ (equation (3.18) of reference [21]) for an electron–phonon system is reduced to

$$\sigma_{rs}(0) = \frac{\hbar}{V} \sum_{\lambda_1,\lambda_2} \langle\lambda_1|j_s|\lambda_2\rangle\langle\lambda_2|j_r|\lambda_1\rangle \frac{f(\varepsilon_1) - f(\varepsilon_2)}{\varepsilon_2 - \varepsilon_1} \frac{\Gamma_{1,2}}{(\varepsilon_1 - \varepsilon_2)^2 + \Gamma_{1,2}^2} \qquad (r, s = x, y, z). \tag{3.1}$$

Here, V is the volume, $f(\varepsilon_i)$ is a Fermi–Dirac distribution function for electrons with energy ε_i associated with the state $|\lambda_i\rangle$, $\hbar$ is the Planck constant divided by 2π, and j_r is the r-component of a single-electron current operator $\boldsymbol{j} = -(e/m)(\boldsymbol{p}+e\boldsymbol{A})$, $-e$ (<0) being the electron charge. The quantity $\Gamma_{1,2}$ is associated with electronic transitions between the states $|\lambda_1\rangle$ and $|\lambda_2\rangle$ effected by absorbing and/or emitting a phonon with an energy $\hbar\omega_q$, and plays the role of the width (collision broadening) in the spectral lineshape. The $\Gamma_{1,2}$ in equation (3.1) is evaluated from the general expression for the electric-field-dependent $\Gamma_{1,2}(E)$ given by equation (3.19a) of reference [21]. For a weak electron–phonon interaction and in the limit of weak electric fields, the expression is

$$\begin{aligned}\Gamma_{1,2} = \pi \sum_{\boldsymbol{q}} \sum_{\lambda_3} \Big[(N_q + 1) \Big\{ |\langle\lambda_2|\gamma_q|\lambda_3\rangle|^2 \delta(\varepsilon_{\lambda_1} - \varepsilon_{\lambda_3} - \hbar\omega_q) + |\langle\lambda_3|\gamma_q^\dagger|\lambda_1\rangle|^2 \\ \times\, \delta(\varepsilon_{\lambda_3} - \varepsilon_{\lambda_2} + \hbar\omega_q) \Big\} + N_q \Big\{ |\langle\lambda_2|\gamma_q^\dagger|\lambda_3\rangle|^2 \delta(\varepsilon_{\lambda_1} - \varepsilon_{\lambda_3} + \hbar\omega_q) \\ + |\langle\lambda_3|\gamma_q|\lambda_1\rangle|^2 \delta(\varepsilon_{\lambda_3} - \varepsilon_{\lambda_2} - \hbar\omega_q) \Big\} \Big]\end{aligned} \tag{3.2}$$

where N_q (=$[\exp(\beta\hbar\omega_q) - 1]^{-1}$) is the Planck distribution function for phonons with energy $\hbar\omega_q$ ($\boldsymbol{q}$ being a 3D wave vector of phonons), $\beta = 1/k_B T$ (k_B being Boltzmann's constant, T the phonon temperature), γ_q is a single-electron–phonon interaction operator given by equation (2.13), and ε_λ is the eigenenergy of an electron in the state $|\lambda\rangle$. It should be noted that equation (3.1) along with equation (3.2) is equivalent to the well-known Kubo formula for an electrical conductivity in an electron–phonon system [20, 22].

To calculate the transverse magnetoconductivity σ_{yy} for the present model systems, we need the matrix elements of the y-component single-electron current operator, j_y ($\equiv j_{y'}$), which is given in the new coordinates by

$$j_{y'} = -\frac{e}{m}(p_{y'} + eA_{y'}) = -\frac{e}{m}(p_{y'} + eBx'). \tag{3.3}$$

In the representation (2.9), we obtain the matrix elements $|\langle n', l', k'_{y'}|j_{y'}|n, l, k_{y'}\rangle|^2$ as

$$|\langle n', l', k'_{y'}|j_{y'}|n, l, k_{y'}\rangle|^2 = \left(\frac{e\hbar k_{y'}}{m}\right)^2 \left(\frac{2\pi}{L_y}\right)^2 \delta_{n',n}\delta_{l',l}\delta(k_{y'} - k'_{y'})$$

$$+\frac{(e\omega_c l_{x'})^2}{2}\left(\frac{2\pi}{L_y}\right)^2[n\delta_{n',n-1}+(n+1)\delta_{n',n+1}]\delta_{l',l}\delta(k_{y'}-k'_{y'}). \tag{3.4}$$

By making use of equations (3.1) and (3.4), the transverse magnetoconductivity σ_{yy} for the present model systems can be expressed as

$$\sigma_{yy}=\frac{4\pi^2\hbar}{VL_y^2}\sum_{\alpha_1,\alpha_2}\left[\frac{e^2\hbar^2k_1^2}{m^2}\delta_{n_2,n_1}+\frac{e^2\omega_c^2l_{x'}^2}{2}\{n_1\delta_{n_2,n_1-1}+(n_1+1)\delta_{n_2,n_1+1}\}\right]\delta_{l_2,l_1}$$
$$\times\,\delta(k_1-k_2)\frac{f(\varepsilon_1)-f(\varepsilon_2)}{\varepsilon_2-\varepsilon_1}\frac{\Gamma_{1,2}}{(\varepsilon_1-\varepsilon_2)^2+\Gamma_{1,2}^2} \tag{3.5}$$

where the notation k_i ($\equiv k_{iy'}$) has been used, and the Fermi–Dirac distribution function $f(\varepsilon_i)$ is associated with the eigenstate $|\alpha_i\rangle$ in equation (2.9) with its eigenenergy ε_i given by equation (2.10). The $\Gamma_{1,2}$ in equation (3.5) can be calculated from equation (3.2) for the present model systems. The matrix elements of $\gamma_{\boldsymbol{q}}$ and $\gamma_{\boldsymbol{q}}^\dagger$ are respectively found with the use of the representation (2.9) to be

$$|\langle n',l',k'_{y'}|\gamma_{\boldsymbol{q}}|n,l,k_{y'}\rangle|^2=\left(\frac{2\pi}{L_y}\right)^2|C(\boldsymbol{q})|^2|\mathcal{J}_{n',n}(u)|^2|\mathcal{J}_{l',l}(v)|^2\delta(q_{y'}+k_{y'}-k'_{y'}) \tag{3.6a}$$

$$|\langle n',l',k'_{y'}|\gamma_{\boldsymbol{q}}^\dagger|n,l,k_{y'}\rangle|^2=\left(\frac{2\pi}{L_y}\right)^2|C(\boldsymbol{q})|^2|\mathcal{J}_{n',n}(u)|^2|\mathcal{J}_{l',l}(v)|^2\delta(q_{y'}-k_{y'}+k'_{y'}) \tag{3.6b}$$

where $|\mathcal{J}_{n',n}(u)|^2$ and $|\mathcal{J}_{l',l}(v)|^2$ are respectively given by

$$|\mathcal{J}_{n',n}(u)|^2=\frac{n_<!}{n_>!}\mathrm{e}^{-u}u^{n_>-n_<}[\mathcal{L}_{n_<}^{n_>-n_<}(u)]^2 \tag{3.7a}$$

$$|\mathcal{J}_{l',l}(v)|^2=\frac{l_<!}{l_>!}\mathrm{e}^{-v}v^{l_>-l_<}[\mathcal{L}_{l_<}^{l_>-l_<}(v)]^2. \tag{3.7b}$$

Here, u, v are given by $u=\frac{1}{2}\{l_{x'}^{-2}(x_0-x'_0)^2+l_{x'}^2q_{x'}^2\}$ and $v=\frac{1}{2}l_{z'}^2q_{z'}^2$, respectively. In equations (3.7a), (3.7b), $\mathcal{L}_n^m(x)$ denotes a Laguerre polynomial [19], $n_>=\max[n,n']$, $n_<=\min[n,n']$, $l_>=\max[l,l']$, and $l_<=\min[l,l']$. By making use of equations (3.6a), (3.6b), and (2.10) in equation (3.2), we obtain the $\Gamma_{1,2}$ in equation (3.5) as

$$\Gamma_{1,2}=\pi\sum_{\boldsymbol{q}}\sum_{\lambda_3}\left(\frac{2\pi}{L_y}\right)|C(\boldsymbol{q})|^2\Big\{(N_{\boldsymbol{q}}+1)\Big[\left|\mathcal{J}_{n_2n_3}(u_2)\right|^2\left|\mathcal{J}_{l_2l_3}(v)\right|^2\delta(q_{y'}+k_3$$
$$-\,k_2)\delta[(n_1-n_3)\hbar\Omega_{x'}+(l_1-l_3)\hbar\Omega_{z'}+\hbar^2(k_1^2-k_3^2)/2\tilde{m}-\hbar\omega_{\boldsymbol{q}}]$$
$$+\,\left|\mathcal{J}_{n_3n_1}(u_1)\right|^2\left|\mathcal{J}_{l_3l_1}(v)\right|^2\delta(-q_{y'}+k_1-k_3)$$
$$\times\,\delta[(n_3-n_2)\hbar\Omega_{x'}+(l_3-l_2)\hbar\Omega_{z'}+\hbar^2(k_3^2-k_2^2)/2\tilde{m}+\hbar\omega_{\boldsymbol{q}}]\Big]\Big\}$$
$$+\,\pi\sum_{\boldsymbol{q}}\sum_{\lambda_3}\left(\frac{2\pi}{L_y}\right)|C(\boldsymbol{q})|^2\Big\{N_{\boldsymbol{q}}\Big[\left|\mathcal{J}_{n_2n_3}(u_2)\right|^2\left|\mathcal{J}_{l_2l_3}(v)\right|^2\delta(-q_{y'}+k_3$$
$$-\,k_2)\delta[(n_1-n_3)\hbar\Omega_{x'}+(l_1-l_3)\hbar\Omega_{z'}+\hbar^2(k_1^2-k_3^2)/2\tilde{m}+\hbar\omega_{\boldsymbol{q}}]$$
$$+\,\left|\mathcal{J}_{n_3n_1}(u_1)\right|^2\left|\mathcal{J}_{l_3l_1}(v)\right|^2\delta(q_{y'}+k_1-k_3)$$
$$\times\,\delta[(n_3-n_2)\hbar\Omega_{x'}+(l_3-l_2)\hbar\Omega_{z'}+\hbar^2(k_3^2-k_2^2)/2\tilde{m}-\hbar\omega_{\boldsymbol{q}}]\Big]\Big\} \tag{3.8}$$

where u_1 and u_2 are respectively given by

$$u_1=\frac{1}{2}[l_{x'}^{-2}(x_1-x_3)^2+l_{x'}^2q_{x'}^2]$$

and

$$u_2 = \frac{1}{2}[l_{x'}^{-2}(x_2 - x_3)^2 + l_{x'}^2 q_{x'}^2]$$

with $x_i = \hbar k_i \omega_c / m\Omega_{x'}^2$. Since we are dealing with the Q1D/Q2DEG formed in the heterointerfaces of semiconductors, the electron density of such systems is customarily very low. In the high-temperature or the non-degenerate limit ($\exp[\beta'(\varepsilon_\alpha - \mu)] \gg 1$) for those confined free electrons, the Fermi–Dirac distribution functions $f(\varepsilon_i)$ ($\equiv f(\varepsilon_{\alpha_i})$) in equation (3.5) can be approximated as a Boltzmann distribution function:

$$f(\varepsilon_\alpha) \approx A \exp\Big[\beta'(\mu - \varepsilon_\alpha)\Big]. \tag{3.9}$$

Here, μ denotes the Fermi energy and $\beta' = 1/k_B T'$, T' being the electron temperature. Note that $T' = T$ ($\beta' = \beta$) holds for the present case since it is assumed that the Q1D/Q2D electronic system is subjected to a weak electric field. The normalization constant A is determined from

$$N_e = \sum_\alpha f(\varepsilon_\alpha) = \frac{L_y}{2\pi} \sum_{n,l} \int \mathrm{d}k_y \ f(\varepsilon_{n,l,k_y})$$

(N_e being the total number of electrons in the system) and is given by

$$A = \frac{(2\pi\beta)^{1/2} N_e \{1 - \exp[-\beta\hbar\Omega_{x'}]\}\{1 - \exp[-\beta\hbar\Omega_{z'}]\}}{L_y \tilde{m}^{1/2} \exp[\beta(\mu - \hbar\Omega_{x'}/2 - \hbar\Omega_{z'}/2)]}. \tag{3.9a}$$

Utilizing equations (3.8) and (3.9) in equation (3.5) and carrying out the α_2-summation (i.e., $\sum_{\alpha_2} \equiv \sum_{n_2,l_2} \sum_{k_2}$) by converting

$$\sum_{\alpha_2} \rightarrow \frac{L_y}{2\pi} \sum_{n_2,l_2} \int \mathrm{d}k_2$$

the conductivity formula (3.5) for the Q1D/Q2D electronic system can be written as

$$\begin{aligned}
\sigma_{yy} = {} & \frac{\hbar}{V} \sum_{n_1,l_1} \int \mathrm{d}k_1 \ \frac{e^2\hbar^2\beta}{m^2} k_1^2 f(\varepsilon_{\alpha_1}) \frac{1}{\Gamma_1^{(1)}} - \frac{\hbar}{V} \sum_{n_1,l_1} \int \mathrm{d}k_1 \ \frac{e^2\omega_c^2 l_{x'}^2}{2\hbar\Omega_{x'}} \\
& \times A \mathrm{e}^{\beta(\mu - \hbar\Omega_{x'}/2 - \hbar\Omega_{z'}/2)} \mathrm{e}^{-\beta n_1 \hbar\Omega_{x'}} (1 - \mathrm{e}^{\beta\hbar\Omega_{x'}}) \mathrm{e}^{-\beta l_1 \hbar\Omega_{z'}} \mathrm{e}^{-\beta\hbar^2 k_1^2/2\tilde{m}} \\
& \times \frac{\Gamma_1^{(2)}}{(\hbar\Omega_{x'})^2 + (\Gamma_1^{(2)})^2} + \frac{\hbar}{V} \sum_{n_1,l_1} \int \mathrm{d}k_1 \ \frac{e^2\omega_c^2 l_{x'}^2}{2\hbar\Omega_{x'}} A \mathrm{e}^{\beta(\mu - \hbar\Omega_{x'}/2 - \hbar\Omega_{z'}/2)} \\
& \times \mathrm{e}^{-\beta n_1 \hbar\Omega_{x'}} (1 - \mathrm{e}^{-\beta\hbar\Omega_{x'}}) \mathrm{e}^{-\beta l_1 \hbar\Omega_{z'}} \mathrm{e}^{-\beta\hbar^2 k_1^2/2\tilde{m}} \frac{\Gamma_1^{(3)}}{(\hbar\Omega_{x'})^2 + (\Gamma_1^{(3)})^2}
\end{aligned} \tag{3.10}$$

where A is given by equation (3.9a). $\Gamma_1^{(1)}$, $\Gamma_1^{(2)}$, $\Gamma_1^{(3)}$ are respectively given by

$$\begin{aligned}
\Gamma_1^{(1)} := {} & \pi \sum_{\boldsymbol{q}} \sum_{n_3,l_3} \int \mathrm{d}k_3 \ \frac{4\pi}{L_y} |C(\boldsymbol{q})|^2 (N_{\boldsymbol{q}} + 1) |\mathcal{J}_{n_1,n_3}(u_1)|^2 |\mathcal{J}_{l_1,l_3}(v)|^2 \delta(q_{y'} + k_3 \\
& - k_1) \delta[(n_1 - n_3)\hbar\Omega_{x'} + (l_1 - l_3)\hbar\Omega_{z'} + \hbar^2(k_1^2 - k_3^2)/2\tilde{m} - \hbar\omega_{\boldsymbol{q}}] \\
& + \pi \sum_{\boldsymbol{q}} \sum_{n_3,l_3} \int \mathrm{d}k_3 \ \frac{4\pi}{L_y} |C(\boldsymbol{q})|^2 N_{\boldsymbol{q}} |\mathcal{J}_{n_1,n_3}(u_1)|^2 |\mathcal{J}_{l_1,l_3}(v)|^2 \delta(q_{y'} + k_1 \\
& - k_3) \delta[(n_3 - n_1)\hbar\Omega_{x'} + (l_3 - l_1)\hbar\Omega_{z'} + \hbar^2(k_3^2 - k_1^2)/2\tilde{m} - \hbar\omega_{\boldsymbol{q}}]
\end{aligned} \tag{3.11}$$

$$\Gamma_1^{(2)} := \pi \sum_{\boldsymbol{q}} \sum_{n_3,l_3} \int \mathrm{d}k_3 \ \frac{2\pi}{L_y} |C(\boldsymbol{q})|^2 (N_{\boldsymbol{q}} + 1) \Big[|\mathcal{J}_{n_1-1,n_3}(u_1)|^2 |\mathcal{J}_{l_1,l_3}(v)|^2 \delta(q_{y'} + k_3$$

$$
\begin{aligned}
&- k_1)\delta[(n_1 - n_3)\hbar\Omega_{x'} + (l_1 - l_3)\hbar\Omega_{z'} + \hbar^2(k_1^2 - k_3^2)/2\tilde{m} - \hbar\omega_{\boldsymbol{q}}] \\
&+ |\mathcal{J}_{n_3,n_1}(u_1)|^2|\mathcal{J}_{l_3,l_1}(v)|^2\delta(-q_{y'} + k_1 - k_3) \\
&\times \delta[(n_3 - n_1 + 1)\hbar\Omega_{x'} + (l_3 - l_1)\hbar\Omega_{z'} + \hbar^2(k_3^2 - k_1^2)/2\tilde{m} + \hbar\omega_{\boldsymbol{q}}]\Big] \\
&+ \pi\sum_{\boldsymbol{q}}\sum_{n_3,l_3}\int \mathrm{d}k_3\,\frac{2\pi}{L_y}|C(\boldsymbol{q})|^2 N_{\boldsymbol{q}}\Big[|\mathcal{J}_{n_1-1,n_3}(u_1)|^2|\mathcal{J}_{l_1,l_3}(v)|^2\delta(-q_{y'} + k_3 \\
&- k_1)\delta[(n_1 - n_3)\hbar\Omega_{x'} + (l_1 - l_3)\hbar\Omega_{z'} + \hbar^2(k_1^2 - k_3^2)/2\tilde{m} + \hbar\omega_{\boldsymbol{q}}] \\
&+ |\mathcal{J}_{n_1,n_3}(u_1)|^2|\mathcal{J}_{l_1,l_3}(v)|^2\delta(q_{y'} + k_1 - k_3) \\
&\times \delta[(n_3 - n_1 + 1)\hbar\Omega_{x'} + (l_3 - l_1)\hbar\Omega_{z'} + \hbar^2(k_3^2 - k_1^2)/2\tilde{m} - \hbar\omega_{\boldsymbol{q}}]\Big]
\end{aligned}
\qquad (3.12)
$$

$$
\begin{aligned}
\Gamma_1^{(3)} := {}& \pi\sum_{\boldsymbol{q}}\sum_{n_3,l_3}\int \mathrm{d}k_3\,\frac{2\pi}{L_y}|C(\boldsymbol{q})|^2(N_{\boldsymbol{q}} + 1)\Big[|\mathcal{J}_{n_1+1,n_3}(u_1)|^2|\mathcal{J}_{l_1,l_3}(v)|^2\delta(q_{y'} + k_3 \\
&- k_1)\delta[(n_1 - n_3)\hbar\Omega_{x'} + (l_1 - l_3)\hbar\Omega_{z'} + \hbar^2(k_1^2 - k_3^2)/2\tilde{m} - \hbar\omega_{\boldsymbol{q}}] \\
&+ |\mathcal{J}_{n_3,n_1}(u_1)|^2|\mathcal{J}_{l_3,l_1}(v)|^2\delta(-q_{y'} + k_1 - k_3) \\
&\times \delta[(n_3 - n_1 - 1)\hbar\Omega_{x'} + (l_3 - l_1)\hbar\Omega_{z'} + \hbar^2(k_3^2 - k_1^2)/2\tilde{m} + \hbar\omega_{\boldsymbol{q}}]\Big] \\
&+ \pi\sum_{\boldsymbol{q}}\sum_{n_3,l_3}\int \mathrm{d}k_3\,\frac{2\pi}{L_y}|C(\boldsymbol{q})|^2 N_{\boldsymbol{q}}\Big[|\mathcal{J}_{n_1+1,n_3}(u_1)|^2|\mathcal{J}_{l_1,l_3}(v)|^2\delta(-q_{y'} + k_3 \\
&- k_1)\delta[(n_1 - n_3)\hbar\Omega_{x'} + (l_1 - l_3)\hbar\Omega_{z'} + \hbar^2(k_1^2 - k_3^2)/2\tilde{m} + \hbar\omega_{\boldsymbol{q}}] \\
&+ |\mathcal{J}_{n_1,n_3}(u_1)|^2|\mathcal{J}_{l_1,l_3}(v)|^2\delta(q_{y'} + k_1 - k_3) \\
&\times \delta[(n_3 - n_1 - 1)\hbar\Omega_{x'} + (l_3 - l_1)\hbar\Omega_{z'} + \hbar^2(k_3^2 - k_1^2)/2\tilde{m} - \hbar\omega_{\boldsymbol{q}}]\Big].
\end{aligned}
\qquad (3.13)
$$

In equation (3.10), the first term expresses the *Drude* term arising from the drift (non-hopping) motion of electrons within the localized states through the electron–phonon interaction. In contrast, the second and the third terms express the *hopping* terms, which are associated with electron hopping motion between the localized (effective Landau and/or sub-band) states effected by absorbing and/or emitting a phonon with an energy $\hbar\omega_{\boldsymbol{q}}$ in the scattering events. In fact, these terms are related to the oscillatory behaviour of MPR effects. Accordingly, we shall denote the transverse magnetoconductivity associated with these hopping terms as σ_{yy}^{MPR} hereafter. In the next section, we shall analyse it in detail in order to get insight into MPR effects in the Q1D and the Q2D electronic systems.

4. Magnetophonon resonances in tilted magnetic fields

Let us consider the case where the applied magnetic field ($\boldsymbol{B}$) is so large that the cyclotron energy $\hbar\omega_c$ is sufficiently larger than the temperature (T) of the system. In the high-temperature (or the non-degenerate limit) and the high-quantum limit ($\hbar\omega_c \gg k_BT$), only one or two magnetic sub-bands (namely, effective Landau levels) are customarily occupied. Accordingly, it may be sufficient for us to consider the electronic transitions between the states specified by $n_i = 0, 1$ and $l_i = 0, 1$ ($i = 1, 2$) in equation (3.5) or (3.10) for the fundamental MPR. When the electrons are in the lowest effective Landau level (namely, when $n_1 = 0$), the term with δ_{n_2,n_1-1} in the conductivity (3.5) becomes zero due to the selection rule (3.4), and does not contribute to the conductivity. Therefore, the conductivity formula (3.5) and hence (3.10) associated with MPR for the Q1D/Q2DEG can be expressed by

$$\sigma_{yy}^{MPR} = \frac{\hbar}{V} \int \mathrm{d}k_1 \ \frac{e^2\omega_c^2 l_{x'}^2}{\hbar\Omega_{x'}} A \mathrm{e}^{\beta(\mu-\hbar\Omega_{x'}/2-\hbar\Omega_{z'}/2-\hbar^2k_1^2/2\tilde{m})}(1-\mathrm{e}^{-\beta\hbar\Omega_{x'}}) \frac{\Gamma_1^{(3)}}{(\hbar\Omega_{x'})^2+(\Gamma_1^{(3)})^2} \tag{4.1}$$

where after carrying out the k_3-integration in equation (3.13), $\Gamma_1^{(3)}$ is given by

$$\begin{aligned}\Gamma_1^{(3)} = \pi \sum_{\boldsymbol{q}} \sum_{n_3,l_3} (2\pi/L_y)|C(\boldsymbol{q})|^2 (N_{\boldsymbol{q}}+1) \Big[|\mathcal{J}_{1,n_3}(u)|^2 |\mathcal{J}_{0,l_3}(v)|^2 \delta[-n_3\hbar\Omega_{x'} - l_3\hbar\Omega_{z'} \\ - \hbar^2(q_{y'}^2 - 2k_1q_{y'})/2\tilde{m} - \hbar\omega_{\boldsymbol{q}}] + |\mathcal{J}_{0,n_3}(u)|^2 |\mathcal{J}_{l_3,0}(v)|^2 \delta[(n_3-1)\hbar\Omega_{x'} \\ + l_3\hbar\Omega_{z'} + \hbar^2(q_{y'}^2 - 2k_1q_{y'})/2\tilde{m} + \hbar\omega_{\boldsymbol{q}}] \Big] + \pi \sum_{\boldsymbol{q}} \sum_{n_3,l_3} (2\pi/L_y)|C(\boldsymbol{q})|^2 \\ \times N_{\boldsymbol{q}} \Big[|\mathcal{J}_{1,n_3}(u)|^2 |\mathcal{J}_{0,l_3}(v)|^2 \delta[-n_3\hbar\Omega_{x'} - l_3\hbar\Omega_{z'} - \hbar^2(q_{y'}^2 + 2k_1q_{y'})/2\tilde{m} \\ + \hbar\omega_{\boldsymbol{q}}] + |\mathcal{J}_{0,n_3}(u)|^2 |\mathcal{J}_{0,l_3}(v)|^2 \delta[(n_3-1)\hbar\Omega_{x'} + l_3\hbar\Omega_{z'} \\ + \hbar^2(q_{y'}^2 + 2k_1q_{y'})/2\tilde{m} - \hbar\omega_{\boldsymbol{q}}] \Big].\end{aligned} \tag{4.2}$$

Here u, v are given by $u = l_{x'}^2(\omega_c^2 q_{y'}^2/\Omega_{x'}^2 + q_{x'}^2)/2$ and $v = l_{z'}^2 q_{z'}^2/2$, respectively. To obtain equations (4.1) and (4.2), we took into account that $l_i = 0, 1$ $(i = 1, 2)$ for the effective (electrostatic) sub-band states in the evaluation of equation (3.5) along with equation (3.8). Since we are considering the MPR effects, where electrons are scattered by LO phonons, we may put $\omega_{\boldsymbol{q}} = \omega_{LO}$ ($\approx$constant), where ω_{LO} is the LO-phonon frequency. Here, we assume that the phonons are dispersionless and bulk (three dimensional). Accordingly, the Planck distribution function $N_{\boldsymbol{q}}$ should be replaced by $N_0 \equiv [\exp(\beta\hbar\omega_{LO}) - 1]^{-1}$ and the Fourier component of the interaction potential $|C(\boldsymbol{q})|^2$ will be replaced by $\hbar D^2/2\rho\omega_{LO}V$ for LO-phonon scattering as was done by several authors [6, 12, 23]. Here, ρ is the bulk density and D is a constant with energy dimensions. In the evaluation of equation (4.2) for bulk LO phonons, we consider the case where $q_{y'} \gg k_1$ since the maximum of the density of states appears at $k_1 = 0$ and so we can set

$$\hbar^2(q_{y'}^2 \pm 2k_1q_{y'})/2\tilde{m} \approx \hbar^2 q_{y'}^2/2\tilde{m}$$

in the calculation of $\Gamma_1^{(3)}$ as an approximation as did Mori *et al* [11]. By converting the sum over $\boldsymbol{q}$ into integrals according to the usual prescription

$$\sum_{\boldsymbol{q}} \to \frac{V}{(2\pi)^3} \int\int\int \mathrm{d}q_{x'}\ \mathrm{d}q_{y'}\ \mathrm{d}q_{z'}$$

in equation (4.2), the equation for $\Gamma_1^{(3)}$ can be analytically evaluated as

$$\begin{aligned}\Gamma_1^{(3)} \approx \Lambda \frac{\Omega_{x'}^2\sqrt{\Omega_{x'}\Omega_{z'}}}{\Omega_{x'}^2 - \Omega_{z'}^2}(N_0+1)\Big[\exp\big[-\kappa(1-\omega_{LO}/\Omega_{x'})\big]\,\Theta(\Omega_{x'}-\omega_{LO}) \\ + \frac{1}{2}\exp\big[-\kappa(1-\Omega_{z'}/\Omega_{x'}-\omega_{LO}/\Omega_{x'})\big]\,\Theta(\Omega_{x'}-\Omega_{z'}-\omega_{LO})\Big] \\ + \Lambda'\frac{\Omega_{x'}^2\sqrt{\Omega_{x'}\Omega_{z'}}}{\Omega_{x'}^2 - \Omega_{z'}^2} N_0 \Big[2\exp\big[-\kappa\omega_{LO}/\Omega_{x'}\big]\,(\kappa\omega_{LO}/\Omega_{x'} + 1/2) \\ + \exp\big[-\kappa(\omega_{LO}/\Omega_{x'} - \Omega_{z'}/\Omega_{x'})\big]\Big(\kappa(\omega_{LO}/\Omega_{x'} - \Omega_{z'}/\Omega_{x'}) + 1/2\Big) \\ \times\ \Theta(\omega_{LO}-\Omega_{z'}) + \exp\big[-\kappa(\omega_{LO}/\Omega_{x'}-1)\big]\Big(3/2 - \kappa(\omega_{LO}/\Omega_{x'}-1)\Big)\end{aligned}$$

$$\times\ \Theta(\omega_{LO} - \Omega_{x'}) + \exp\left[-\kappa(\omega_{LO}/\Omega_{x'} - 1 - \Omega_{z'}/\Omega_{x'})\right]$$
$$\times\ \Big(1/4 - \kappa(\omega_{LO}/\Omega_{x'} - 1 - \Omega_{z'}/\Omega_{x'})/2\Big)\Theta(\omega_{LO} - \Omega_{x'} - \Omega_{z'})$$
$$+\ \exp\left[-\kappa(\omega_{LO}/\Omega_{x'} + 1)\right] + \frac{1}{2}\exp\left[-\kappa(\omega_{LO}/\Omega_{x'} + 1 - \Omega_{z'}/\Omega_{x'})\right]$$
$$\times\ \Theta(\omega_{LO} + \Omega_{x'} - \Omega_{z'})\Big] \tag{4.3}$$

where $\Lambda = m^2 D^2/2L_y\hbar^2\rho\omega_{LO}$, $\kappa = \omega_c^2/(\Omega_{x'}^2 - \omega_c^2)$, and $\Theta(x)$ denotes a step function. Since this equation does not depend on k_1, we can easily perform the k_1-integration in equation (4.1) and obtain σ_{yy}^{MPR} as

$$\sigma_{yy}^{MPR} = \frac{\pi\hbar e^2 n_e}{mL_y}\left(\frac{\omega_c}{\Omega_{x'}}\right)^2(1 - \mathrm{e}^{-\beta\hbar\Omega_{x'}})^2(1 - \mathrm{e}^{-\beta\hbar\Omega_{z'}})\frac{\Gamma_1^{(3)}}{(\hbar\Omega_{x'})^2 + (\Gamma_1^{(3)})^2} \tag{4.4}$$

where $\Gamma_1^{(3)}$ is given by equation (4.3) and n_e denotes the electron density in the Q1D/Q2D system with appropriate dimensions. It should be noted that equation (4.4) along with equation (4.3) forms the basic equation for the MPR spectral lineshape for analysing MPR effects in the Q1D/Q2D electronic system under tilted strong magnetic fields. $\Gamma_1^{(3)}$ plays an important role in determining the height and width of the MPR peaks as well as their peak positions.

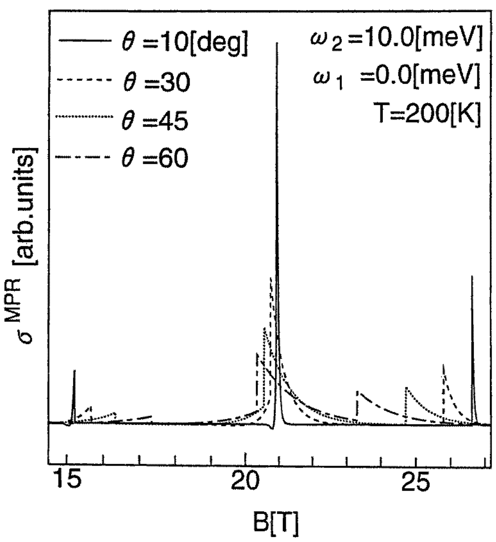

Figure 1. The dependence on the magnetic field (B) of the magnetoconductivity (σ_{yy}^{MPR}) for different tilt angles (θ). (Q2D.)

5. Results and discussion

We have obtained the magnetoconductivity formula σ_{yy}^{MPR} associated with MPR for the Q2D/Q1D electronic system on the basis of the model described in section 2. By making use of equation (4.4) along with equation (4.3), the spectral lineshapes for σ_{yy}^{MPR} in the Q2D/Q1D system are plotted in figures 1 and 2 as functions of magnetic field B for different

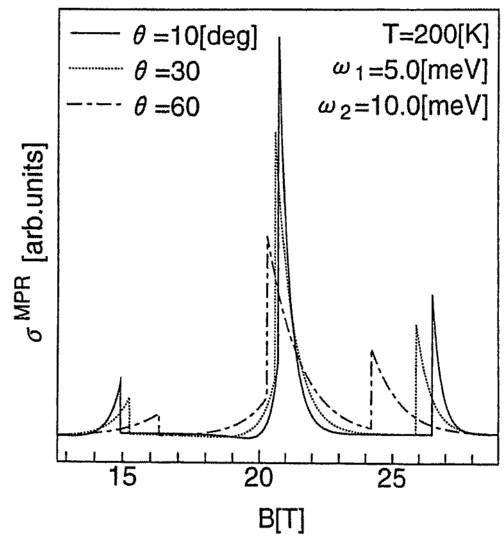

Figure 2. The dependence on the magnetic field (B) of the magnetoconductivity (σ_{yy}^{MPR}) for different tilt angles (θ). (Q1D.)

tilt angles θ of the transverse tilted magnetic field $\boldsymbol{B} = (-B\sin\theta, 0, B\cos\theta)$ applied to the electronic wire/plane. In these figures, we can see the following features for the Q2D/Q1D system:

(i) there are three peaks in $\sigma_{yy}^{MPR}(\boldsymbol{B})$;

(ii) with the increase of the tilt angle θ of the applied magnetic field, the peak in the weak side of the magnetic field, the resonant magnetic fields, shifts to the higher side whereas the peaks in the middle and the higher side of the field shift to the lower-field side; and

(iii) with the increase of the tilt angle θ, the height of these peaks decreases and their resonance widths broaden.

Let us first examine feature (i). Since MPR is a phenomenon which occurs in the electronic system subjected to quantizing magnetic fields, it is sufficient for us to consider the case where the cyclotron energy always exceeds the energy of a confining potential since this condition is customarily satisfied under normal operating conditions. Here we assumed that the energy of a confining potential could not be equal to a LO-phonon energy. Then there are four possible cases which change $\Gamma_1^{(3)}$ in equation (4.3) abruptly when we vary the tilt angle θ of the applied $\boldsymbol{B}$-field. Those are the terms with the step functions given by $\Theta(\Omega_{x'} - \omega_{LO})$, $\Theta(\Omega_{x'} - \Omega_{z'} - \omega_{LO})$, $\Theta(\omega_{LO} - \Omega_{x'})$, and $\Theta(\omega_{LO} - \Omega_{x'} - \Omega_{z'})$. The abrupt change of $\Gamma_1^{(3)}$ is expected to occur at the magnetic field for which the relaxation time changes abruptly. By inspecting equation (4.4) along with equation (4.3), the conditions for MPR, which give the peak positions (i.e., resonant magnetic fields (B_{peak})) in the spectral lineshape, are actually given by the following three cases:

$$\Omega_{x'} + \Omega_{z'} = \omega_{LO} \qquad \Omega_{x'} = \omega_{LO} \qquad \Omega_{x'} - \Omega_{z'} = \omega_{LO}. \tag{5.1}$$

Here, $\Omega_{x'}$ is given by equation (2.6*a*) and $\Omega_{z'}$ by equation (2.6*b*) in which $\omega_1 = 0$ should be taken for the Q2D system. It is clear that the reason that subsidiary peaks appear ($\Omega_{x'} \pm \Omega_{z'} = \omega_{LO}$) is the presence of $\Omega_{z'}$ in equation (5.1) (unlike in the 3D case) in $\sigma_{yy}^{MPR}(\boldsymbol{B})$ for the Q2D/Q1D system. When the applied magnetic field is tilted by an angle

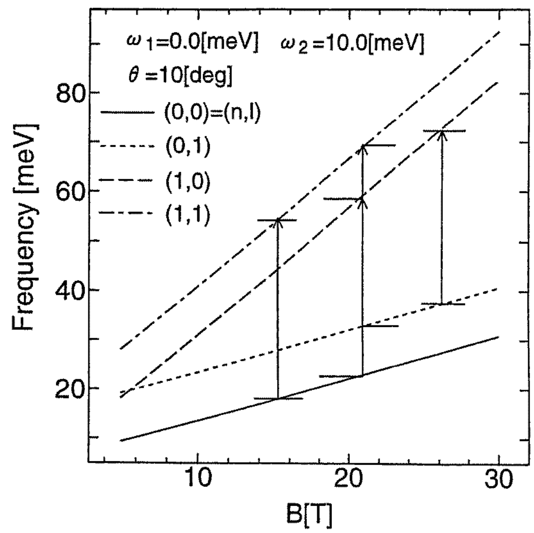

Figure 3. The dependence on the magnetic field (B) of the electronic energy levels ($\varepsilon_{n,l,k_y\approx 0}$). (Q2D.) The MPR conditions (5.1) are satisfied when the vertical transitions $(n, l) = (0, 0) \rightarrow (1, 1)$, $(0, 0) \rightarrow (1, 0)$, $(0, 1) \rightarrow (1, 1)$, and $(0, 1) \rightarrow (1, 1)$ take place via the absorbing of phonon energy $\hbar\omega_{LO}$.

θ, electrons confined in $V(x, z)$ actually 'feel' not only the effective confining potential $m\Omega_{x'}^2(x' + x_0)^2/2$ in the x'-direction but also the effective confining potential $m\Omega_{z'}^2 z'^2/2$ in the z'-direction. In the course of scattering events, the electrons in the effective Landau and sub-band levels specified by the level indices (n, l) could make transitions to one of the effective Landau and sub-band levels (n', l') by absorbing the LO-phonon energy $\hbar\omega_{LO}$ when the conditions (5.1) are satisfied. The first condition indicates processes in which quasi-electrons having respective energies of $\hbar\Omega_{x'}$ and $\hbar\Omega_{z'}$ are created by the absorbing of a LO phonon with energy $\hbar\omega_{LO}$. The second condition indicates a process in which only a quasi-electron with energy $\hbar\Omega_{x'}$ is created by the absorbing of the same phonon energy. The third condition indicates processes in which, via the absorbing of a LO phonon with the same energy, a quasi-electron with energy $\hbar\Omega_{x'}$ is created and a quasi-electron with energy $\hbar\Omega_{z'}$ is however annihilated. To see the physics involved in these processes, for the sake of simplicity, we plotted the electronic energy levels (2.10) (at $k_{y'} \approx 0$) for the Q2D system, specified by the effective Landau and sub-band level indices n, l (=0, 1) as a function of the applied magnetic field (see figure 3). It is evident from a glance at figure 3 that the first condition in equation (5.1) corresponds to the electronic transition from $(n, l) = (0, 0)$ to $(1, 1)$ and the second condition corresponds to the electronic transition either from $(0, 0)$ to $(1, 0)$ or from $(0, 1)$ to $(1, 1)$. The third condition corresponds to the electronic transition from $(0, 1)$ to $(1, 0)$ effected by absorbing a LO phonon with energy $\hbar\omega_{LO}$. The subsidiary MPR positions for the Q2D case given by the conditions $\Omega_{x'} + \Omega_{z'} = \omega_{LO}$ and $\Omega_{x'} - \Omega_{z'} = \omega_{LO}$ essentially correspond to those of Mori *et al* (equation (3) in reference [7]) who considered the case in which the magnetic field is applied perpendicular to the Q2D electronic plane. It should be noted that unlike in the case of MPR in a 3D electronic system (where only one resonant peak appears at $\Omega_{x'} \equiv \omega_c = \omega_{LO}$ when $P = 1$) [14–17], an additional two subsidiary peaks will appear at $\Omega_{x'} \pm \Omega_{z'} = \omega_{LO}$—in addition to the central peak specified by $\Omega_{x'} = \omega_{LO}$—in the Q2D (also Q1D) electronic

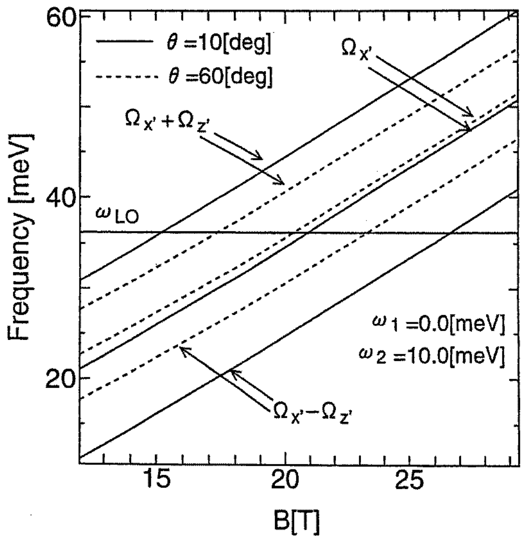

Figure 4. The dependence on the tilt angle of the MPR conditions given by equations (5.1). (Q2D.) The intersections of two lines indicating ω_{LO} and $\Omega_{x'}$, $\Omega_{x'} \pm \Omega_{z'}$ give the resonant magnetic fields (B_{peak}), that is, the MPR peak positions.

system due to the presence of the effective confining potential $m\Omega_{z'}^2 z'^2/2$. The appearance of these subsidiary peaks in the MPR lineshape seems to be a characteristic feature in Q2D as well as Q1D electronic systems.

Next we consider feature (ii). The shift of the resonant peaks in $\sigma_{yy}^{MPR}(\boldsymbol{B})$ for different tilt angles seen in figures 1 and 2 can be understood in terms of the behaviour of $\Omega_{x'}$ and $\Omega_{x'} \pm \Omega_{z'}$ as functions of the magnetic field B at different tilt angles (θ). Again, we consider the Q2D case. Figure 4 indicates the variation of those resonant frequencies, $\Omega_{x'}$ and $\Omega_{x'} \pm \Omega_{z'}$, at different tilt angles. In this figure, the quantities $\Omega_{x'}$ and $\Omega_{x'} \pm \Omega_{z'}$ intercept ω_{LO} at the resonant magnetic field values. In the Q2D system, since $\omega_1 = 0$, $\Omega_{x'}$ and $\Omega_{z'}$ given by equations (2.6*a*) and (2.6*b*) become

$$\Omega_{x'} = \sqrt{\omega_c^2 + \omega_2^2 \sin^2\theta} \qquad \text{and} \qquad \Omega_{z'} = \omega_2 \cos\theta \tag{5.2}$$

respectively. Therefore, for a given value of magnetic field (i.e., ω_c), it is clear from equation (5.2) that the magnitude of $\Omega_{x'}$ always increases whereas that of $\Omega_{z'}$ always decreases with the increase of the tilt angle $\theta \in (0, \pi/2)$. This implies that the constraint on the electron motion (namely, the effective confinement of an electron) in the x'-direction becomes stronger whereas that in the z'-direction becomes weaker when the tilt angle θ increases. Accordingly, $\Omega_{x'} + \Omega_{z'}$ decreases whereas $\Omega_{x'}$ and $\Omega_{x'} - \Omega_{z'}$ increase. These variations due to the increase of the tilt angle can be clearly seen in figure 4 as a shift of the line indicating $\Omega_{x'} + \Omega_{z'}$ downwards (i.e., to the lower-frequency side) and the lines indicating $\Omega_{x'}$ and $\Omega_{x'} - \Omega_{z'}$ upwards (i.e., to the higher-frequency side). Therefore it can be understood that the resonant point (B_{peak}) for the subsidiary peak on the low-field side determined from the condition $\Omega_{x'} + \Omega_{z'} = \omega_{LO}$ shifts to the corresponding point on the higher-field side. The resonant points for the central peak given by $\Omega_{x'} = \omega_{LO}$ and for the subsidiary peak on the high-field side given by $\Omega_{x'} - \Omega_{z'} = \omega_{LO}$ shift to the corresponding points on the lower-field side when the tilt angle θ is increased. See also figure 5, which shows the variation of the resonant magnetic field (B_{peak}) against the tilt angle (θ) of the

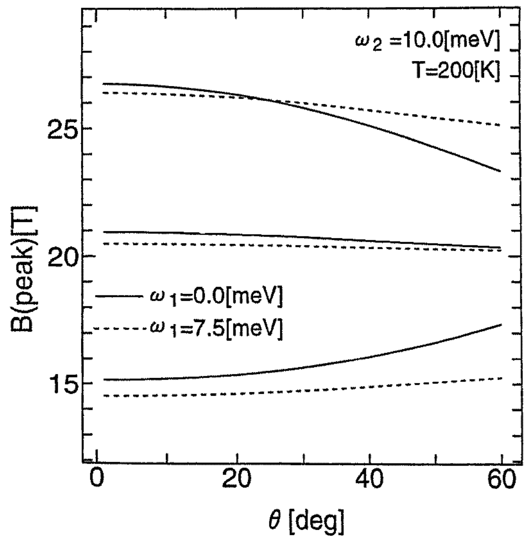

Figure 5. The dependence on the tilt angle (θ) of the resonant magnetic fields (B_{peak}). The solid (dotted) line indicates the Q2D (Q1D) case.

applied magnetic fields in the Q2DEG and the Q1DEG systems. It is clearly seen in this figure that the shift of each MPR peak (for the resonant magnetic field) in the Q1D case (dotted line) is smaller than that of the corresponding peaks in the Q2D case (solid line). This indicates that the tilt-angle dependency on the effective confining-potential frequencies $\Omega_{x'}$ and $\Omega_{z'}$ in the Q1D system is weakened since these confinement frequencies (see equations (2.6*a*), (2.6*b*)) in the Q1D system are more symmetric (with respect to the y-axis) than their counterparts (see equation (5.2)) in the Q2D system due to the presence of the confining potential $m\omega_1^2 x^2/2$. This can be easily understood by considering the special case for a symmetric quantum wire, where the confining-potential frequencies ω_1, ω_2 are given by $\omega_1 = \omega_2 \equiv \omega_0$. Then, equations (2.6*a*) and (2.6*b*) are respectively given by

$$\Omega_{x'} = \sqrt{\omega_0^2 + \omega_c^2} \qquad \text{and} \qquad \Omega_{z'} = \omega_0 \tag{5.3}$$

which do *not* depend on the tilt angle at all. It is noteworthy that the condition $\Omega_{x'} = \omega_{LO}$ (equation (5.2)) for the Q2D system, obtained in this paper, is essentially equivalent to the MPR condition derived by Vasilopoulos *et al* [10] for a Q1DEG system when their Ω is replaced by $\omega_2 \sin\theta$.

The feature (iii) can be explained as follows. The height and width of the MPR peaks seen in figures 1 and 2 are mainly determined by the behaviour of Γ since it appears in terms of the collision broadening due to the electron–phonon interaction and plays the role of the width in the spectral lineshape [20–22]. Increasing the tilt angle of the applied magnetic fields further constrains electron motion since the effective confinement becomes tighter in both Q2D and Q1D systems. Accordingly, we can expect that the frequency of collisions between electrons and LO phonons increases, resulting in the increase of Γ. In fact, with the increase of Γ, the widths of the MPR spectral lineshape in equation (4.4) become wider and its heights (magnitude) lower as seen in figures 1 and 2.

So far we have seen the effect of tilted magnetic fields, namely, the θ-dependency of MPR. Now let us consider the Q1D case, where special attention is paid to the effect of symmetry (with respect to the y-axis) of the quantum wires (or the dimensionality) on MPR.

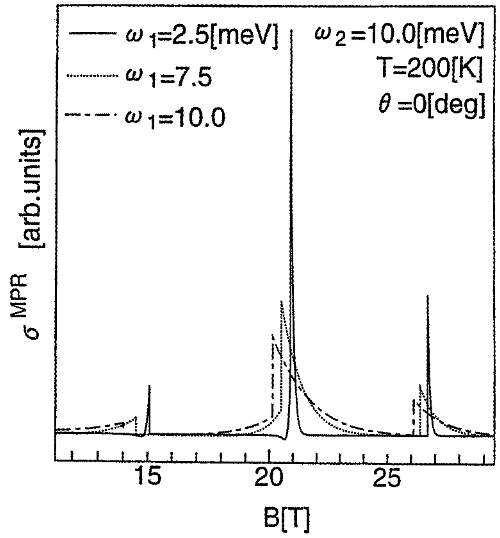

Figure 6. The dependence on the magnetic field (B) of the magnetoconductivity (σ_{yy}^{MPR}) for change of the confining-potential strength ω_1 in the x-direction. (Q1D.)

In other words, we consider the effect of electrostatic confining potentials (characterized by ω_1, ω_2) on MPR since those MPR peak positions and the MPR lineshapes would be influenced by the strength of these confining-potential parameters. To simplify the discussion to see the effect of the strength of the confining potentials on the MPR, we shall consider the case for $\theta = 0$, where magnetic fields are applied normal to the wire. In this case, the MPR conditions (5.1) for the confined electrons (Q1DEG) are reduced to

$$\sqrt{\omega_1^2 + \omega_c^2} + \omega_2 = \omega_{LO} \qquad \sqrt{\omega_1^2 + \omega_c^2} = \omega_{LO} \qquad \sqrt{\omega_1^2 + \omega_c^2} - \omega_2 = \omega_{LO} \tag{5.4}$$

respectively. Figure 6 shows the variation of $\sigma_{yy}^{MPR}(\boldsymbol{B})$ against the strength of one of the confining potentials, ω_1, for the crossed field configuration ($\theta = 0$) (i.e., magnetic fields are applied perpendicular to the wire). On increasing the confinement parameter ω_1 (that is, on making the confinement tighter in the x-direction), all three MPR peaks shift to the lower-B side, and the height of these MPR peaks becomes lower and their widths broader as seen in this figure. This agrees qualitatively with the result of Vasilopoulos *et al* [10] for Q1D quantum wires modelled in terms of the vertical confinement with a triangular well and the lateral one with a parabolic potential. The reason that these MPR peaks shift to smaller magnetic fields (i.e., the lower-field side) is that only the constraint in the x-direction (ω_1) changes. The constraint in the z-direction (ω_2) does not change at all in the present case (see equation (5.4)). Accordingly, in the present case, $\Omega_{z'}$ ($=\omega_2$) does not change but the effective confinement frequency $\Omega_{x'}$ ($=\sqrt{\omega_1^2 + \omega_c^2}$) takes larger values with the increase of ω_1. Therefore, all three MPR peaks given by the conditions (5.4) are expected to shift to smaller magnetic fields (that is, the lower-B side) as the system becomes more one dimensional. It should be noted that when the confinement in the z-direction is tighter (i.e., with the increase of ω_2 rather than ω_1), the Q2D nature of shifting of the MPR peaks appears. That is, the subsidiary peak in the lower magnetic fields shifts to the lower-B side whereas the subsidiary peak in the higher fields shifts to the higher-B side. The central peak does not shift irrespective of the change in ω_2, as discussed before.

We have seen that with the increase of the tilt angle (in the Q2D/Q1D system) (cf. figures 1, 2, and 5) or with the increase of the constraint in one of the confining potentials (in the Q1D system) (cf. figure 6), MPR peaks decrease in height and are broadened. The peak width and height are mainly determined by the Lorentzian spectrum function in equation (4.5) through the behaviour of Γ. Since the quantity Γ is proportional to the inverse of the electronic relaxation time, an increase of Γ leads to the relaxation time becoming shorter due to the collisions (scattering). The increase of Γ, that is, the decrease of the relaxation time, brought about by tilting the applied magnetic fields and/or by tightening the confining potential results in the increase in the frequency of the collisions between electrons and phonons. This is because the electrons are confined in a narrower region when these constraints are stronger. According to the experimental results of Brummell *et al* [4] for Q2D electronic systems, all of the MPR peaks shift to the higher-B side, their peak heights decrease, and their widths broaden when the tilt angle of the applied magnetic fields is increased. Therefore our theoretical results for the Q2D case agree qualitatively with their experimental results as far as the MPR peak heights and their widths are concerned. However, our theoretical result concerning MPR peak shifting does not agree with their experimental results. This disagreement may be due to the fact that their experiment was performed under magnetic fields up to 10 T whereas our calculations were carried out for magnetic fields of above 15 T, taking into account only the effective Landau and sub-band states with $n = 0, 1$ and $l = 0, 1$. Since the MPR peak on the lower-B side shifts to the higher-B side even in the present calculations, we might expect the present theory to reproduce their experimental results qualitatively if we take into account the electronic transitions up to the second excited levels and obtain the MPR conditions valid under magnetic fields up to 10 T. So far we are not aware of any relevant experimental work relating to MPR on the dependence of the tilted magnetic field on σ_{yy}^{MPR} for Q1D electronic systems. It should be noted that our theoretical results are based on a model with a parabolic confining potential. For usual heterostructures it is well known that the confinement potential in the z-direction is far from being parabolic, and it is often approximated as a triangular potential [10, 12]. For a direct comparison with experiments, realistic modelling with the correct confinement potential would be required. We believe however that utilizing a model with a parabolic confinement is good enough for extracting the essential physics of MPR effects in Q2D and Q1D electronic systems in tilted magnetic fields. In other words, the difference between the energy spectra obtained using quasi-triangular potentials and parabolic potentials does not alter the essential physics of MPR effects in Q2D and Q1D electronic systems as far as the fundamental ($P = 1$) MPR, which we considered here, is concerned. Finally, we should comment on a possible influence of electron–electron scattering on MPR. The effect of electron–electron interaction can be taken into account approximately by dividing the bare interactions by the purely electronic contribution to the static wave-vector-dependent dielectric constant $\epsilon(\boldsymbol{q})$. Horing [24] has evaluated this electronic dielectric constant in the random-phase approximation including the effects of magnetic fields. His result may be expressed as $\epsilon(\boldsymbol{q}) = \epsilon(1 + \lambda^2(\boldsymbol{q})/q^2)$, where ϵ and $\lambda(\boldsymbol{q})$ are the high-frequency dielectric constant and the inverse screening length. The explicit expression for $\lambda(\boldsymbol{q})$ is too cumbersome to give here [25], but the electron–phonon interaction $C(\boldsymbol{q})$ in equation (4.2) may be replaced by a screened electron–phonon interaction $C(\boldsymbol{q}) = \mathrm{i}D\hbar^{1/2}/(2\rho\omega_{LO}V)^{1/2}(1 + \lambda^2(\boldsymbol{q})/q^2)$, since the inverse screening length $\lambda(\boldsymbol{q})$ depends on the electron density n_e, which in general depends on temperature T and the magnetic field $\boldsymbol{B}$. Therefore, we would expect the screening to be significant only if the electron density n_e exceeded a critical value $n_{cr}(T, \boldsymbol{B})$. In this case, the effects of electron–electron scattering would be significant, the relaxation rate $\Gamma_1^{(3)}$ would be changed, and the MPR lineshape as well as the MPR linewidth would be affected by electron–electron scattering.

Despite the above shortcomings of the theory, we believe that the simple model that we presented captures qualitatively the essential physics of MPR in Q2D and Q1D electronic systems brought about by the electron confinement due to the electrostatic potentials and the magnetic confinement on tilting a magnetic field. We hope that new experiments will test the validity of our prediction.

Acknowledgments

One of the authors (AS) thanks Professor S Fujita and many members of the Department of Physics, SUNY at Buffalo, for their kind hospitality during the period in which part of this paper was written. The valuable comments and suggestions from Dr D Beachey are gratefully acknowledged.

Appendix. Diagonalization of equation (2.3)

Let us express equation (2.3) with equation (2.4) as

$$h_e = \frac{1}{2m}(p_{x'}^2 + p_{y'}^2 + p_{z'}^2) + \omega_c x' p_{y'} + \frac{m}{2}(ax'^2 + 2bx'z' + cz'^2) \tag{A.1}$$

where a, b, c are given by $a = \omega_1^2 \cos^2\theta + \omega_2 \sin^2\theta + \omega_c^2$, $b = (\omega_2^2 - \omega_1^2)\cos\theta\sin\theta$, $c = \omega_1^2 \sin^2\theta + \omega_2 \cos^2\theta$, respectively. In order to diagonalize (A.1), we would like to obtain the eigenvalue λ of the matrix

$$\mathbf{A} = \begin{pmatrix} a & b \\ b & c \end{pmatrix}. \tag{A.2}$$

The eigenvalue equation is given by

$$\lambda^2 - (a + c)\lambda + (ac - b^2) = 0. \tag{A.3}$$

By solving (A.3), we can obtain the eigenvalue λ as

$$\begin{aligned}\lambda &= \frac{1}{2}\left\{(a+c) \pm \sqrt{(a+c)^2 - 4(ac - b^2)}\right\} \\ &= \frac{1}{2}\left\{(\omega_1^2 + \omega_2^2 + \omega_c^2) \pm \sqrt{(\omega_1^2 - \omega_2^2 + \omega_c^2\cos 2\theta)^2 + \omega_c^4 \sin^2 2\theta}\right\} \\ &\equiv \Omega_\pm^2.\end{aligned} \tag{A.4}$$

Utilizing the coordinate transformations $\{R_{y'}(\phi)|(x', y', z') \mapsto (x'', y'', z'')\}$ effected by rotating the coordinates x' and z' by an angle ϕ with respect to the y'-axis (= the y''-axis), i.e.,

$$\begin{pmatrix} x' \\ y' \\ z' \end{pmatrix} = \begin{pmatrix} \cos\phi & 0 & -\sin\phi \\ 0 & 1 & 0 \\ \sin\phi & 0 & \cos\phi \end{pmatrix} \begin{pmatrix} x'' \\ y'' \\ z'' \end{pmatrix} \tag{A.5}$$

in (A.1), equation (2.3) can be expressed as

$$h_e = \frac{1}{2m}(p_{x''}^2 + p_{y''}^2 + p_{z''}^2) + \omega_c p_{y''}(x''\cos\phi - z''\sin\phi) + \frac{m}{2}\Omega_+^2 x''^2 + \frac{m}{2}\Omega_-^2 z''^2 \tag{A.6}$$

where $\cos\phi$ and $\sin\phi$ are

$$\cos\phi \equiv \frac{\Omega_+^2 - c}{\sqrt{(\Omega_+^2 - c)^2 + b^2}} \qquad \sin\phi \equiv \frac{b}{\sqrt{(\Omega_+^2 - c)^2 + b^2}}. \tag{A.7}$$

Accordingly, the angle of rotation ϕ is related to the confining-potential parameters as well as the tilt angle θ of the applied magnetic field $\boldsymbol{B}$:

$$\tan\phi = \frac{(\omega_2^2 - \omega_1^2)\sin 2\theta}{(\omega_1^2 - \omega_2^2)\cos 2\theta + \omega_c^2 + \sqrt{(\omega_1^2 - \omega_2^2 + \omega_c^2\cos 2\theta)^2 + \omega_c^4 \sin^2\theta}}. \tag{A.8}$$

In the case where $\omega_1, \omega_2 \ll \omega_c$, equations (A.4) and (A.8) can be approximated as

$$\Omega_\pm^2 \simeq \frac{1}{2}\{(\omega_1^2 + \omega_2^2 + \omega_c^2) \pm (\omega_c^2 + \omega_1^2\cos 2\theta - \omega_2^2\cos 2\theta)\} \tag{A.9}$$

and

$$\tan\phi \simeq 0 \tag{A.10}$$

respectively. From (A.10), $\phi \simeq 0$. Thus, equation (A.5) expresses identical transformations. Therefore, equation (A.6) can be expressed by equation (2.5) in the case where $\omega_1, \omega_2 \ll \omega_c$, if we notice that $\Omega_+ \to \Omega_{x'}$ and $\Omega_- \to \Omega_{z'}$ in (A.6).

References

[1] Tsui D C, Englert Th, Cho A Y and Gossard A C 1980 *Phys. Rev. Lett.* **44** 341
[2] Kido G, Miura N, Ohno H and Sakaki H 1982 *J. Phys. Soc. Japan* **51** 2168
[3] Brummell M A, Nicholas R J, Hopkins M A, Harris J J and Foxon C T 1987 *Phys. Rev. Lett.* **58** 77
[4] Brummell M A, Leadley D R, Nicholas R J, Harris J J and Foxon C T 1988 *Surf. Sci.* **196** 451
[5] Noguchi H, Sakaki H, Takamasu T and Miura N 1992 *Phys. Rev.* B **45** 12 148
[6] Vasilopoulos P 1986 *Phys. Rev.* B **33** 8587
[7] Mori N, Taniguchi K, Hamaguchi C, Sasa S and Hiyamizu S 1988 *J. Phys. C: Solid State Phys.* **21** 1791
[8] Leadley D R, Nicholas R J, Singleton J, Xu W, Peeters F M, Devreese J T, van Bockstal L, Herlach F, Perenboom J A A J, Harris J J and Foxon C T 1994 *Surf. Sci.* **305** 327
[9] Suzuki A 1992 *Phys. Rev.* B **45** 6731
[10] Vasilopoulos P, Warmenbol P, Peeters F M and Devreese J T 1989 *Phys. Rev.* B **40** 1810
[11] Mori N, Momose H and Hamaguchi C 1992 *Phys. Rev.* B **45** 4536
[12] Ryu J Y, Hu G Y and O'Connell R F 1994 *Phys. Rev.* B **49** 10 437
[13] Berthold G, Smoliner J, Gornik E, Böhm G, Weimann G, Suski T, Wisniewski P, Hamaguchi C, Mori N and Momose H 1994 *Surf. Sci.* **305** 637
[14] Gurevich V L and Firsov Yu A 1961 *Sov. Phys.–JETP* **13** 137
[15] Firsov Yu A, Gurevich V L, Parfeniev R V and Shalyt S S 1964 *Phys. Rev. Lett.* **12** 660
[16] Stradling R A and Wood R A 1968 *J. Phys. C: Solid State Phys.* **1** 1711
[17] Barker J R 1972 *J. Phys. C: Solid State Phys.* **5** 1657
[18] Suzuki A 1993 *Physica* B **183** 191
[19] Gradshteyn I S and Ryzhik I M 1965 *Tables of Integrals, Series and Products* (New York: Academic)
[20] Suzuki A and Dunn D 1982 *Phys. Rev.* A **25** 2247
[21] Suzuki A 1989 *Phys. Rev.* B **40** 5632
[22] Kubo R, Miyake S J and Hashitsume N 1965 *Solid State Physics* vol 17, ed F Seitz and D Turnbull (New York: Academic) p 269
[23] Vasilopoulos P, Charbonneau M and Van Vliet C M 1987 *Phys. Rev.* B **35** 1334
[24] Horing N J 1969 *Ann. Phys., NY* **54** 409
[25] Dunn D and Suzuki A 1984 *Phys. Rev.* B **29** 942